Journal of Engineering Science and Technology
Vol. 13, No. 7 (2018) 1939 - 1958

CONTINUOUS MOTION NOMINAL CHARACTERISTIC TRAJECTORY FOLLOWING CONTROL FOR POSITION CONTROL OF AN AC DRIVEN X-Y BALL SCREW MECHANISM

S.-H. CHONG*, W.-K. HEE, N. HASIM

Centre of Excellence for Robotics and Automation,
Faculty of Electrical Engineering, Universiti Teknikal Malaysia Melaka,
76100 Hang Tuah Jaya, Durian Tunggal, Melaka, Malaysia
*Corresponding Author: horng@utem.edu.my

Abstract

AC servo mechanisms are widely used in industrial application due to its advantages in higher efficiency, less maintenance, and smoother operation than DC servo mechanism. However, AC servomechanism frequently suffers from its inherently non-linear characteristics and more difficult to be controlled in positioning applications. A general step input easily drove the mechanism and stop smoothly in the open-loop environment, however, it is not the same for AC driven ball screw mechanism. Hence, the contributions in this paper are: (1) the realization of the practical control method - continuous motion nominal characteristic trajectory following (CM NCTF) control to an AC driven ball screw mechanism, (2) the design of a suitable input signal that produces sufficient rapid and smooth response during deceleration motion in the open-loop experiment. The open-loop responses used to construct nominal characteristic trajectory (NCT) are important because it significantly affects the reference following characteristic of the control system. The experimental evaluations were carried out for CM NCTF control system and PI-D control system. The results show that the designed input signal has successfully produced rapid and smooth open-loop responses during deceleration that benefit the reference position near NCT origin. Besides that, the CM NCTF control system that designed with the newly constructed NCT has demonstrated better positioning results than the PI-D controller with almost 10 times of motion error reduction for Y-axis for both amplitudes of 5 mm and 10 mm respectively.

Keywords: AC-driven ball screw, CM-NCTF, Positioning performance, Sensitivity, Practical control, Robustness.

1. Introduction

Servo motor is commonly applied in mechanical systems such as metal cutting and metal forming machines, computer numerical control (CNC) machine, and conveyor belt system. Servo motor can be categorized into two categories, first is DC servo motor and second is AC servo motor. AC servo mechanisms are widely used in industrial application due to its advantages in higher efficiency, less maintenance, fewer stability problems and smoother operation over the DC servo mechanism. However, the AC servomechanism frequently suffers from its inherently non-linear characteristics and more difficult to be controlled in positioning applications.

Position control system in industries has high demands on positioning performance in order to maintain quality and quantity of products. Most of the industrial mechanisms usually operate at high speed for high productivity. Practical controller is always a solution that needed in the industry because it has a simple control structure, easy to design, high adaptively, and robust to the change of plant parameters.

Proportional integral derivative (PID) control systems are widely used as a basic control technology in the industrial control system nowadays, due to the well-known simple control structure, which composed of proportional (P), integration (I), and differential (D) operation. Traditional PID control has mainly controlled the model of the linear process, in fact, the majority of the mechanisms used in the industry has non-linear characteristics, which are usually represented by friction. Sometimes the model of the plant is difficult or cannot be established in the mathematical model. Furthermore, the tuning of PID control systems is not always easy, because of its simple control structure for wide classes of industrial control processes [1, 2].

Recently, several researchers had examined the effectiveness of conventional PID control versus advance PID control system in ball screw mechanism or AC drive mechanism. The advance PID control system used such as non-linear PID control, P/PI control non-linear PID control cascade with feedforward [3, 4], and fuzzy PID control [5]. These researchers prove that the advance PID control has better positioning performance as compared to the conventional PID control when the control system is applied to a non-linear mechanism.

Advanced controllers have been proposed to achieve better positioning performance in the ball screw mechanism. Disturbance observer with variable structure controller has overcome deficiencies due to friction and disturbances [6]. Besides that, back-stepping and hybrid sliding mode controllers were proposed to improve the performance of the system used [6-8]. Reinforcement Learning methods learning the feedback controller of a ball screw feed drive is used in [9] can be an alternative to typical feedback control approaches such as PID controllers. Although these advance controllers are able to show good performance in the robustness of precision positioning, the determination of the unknown in the model parameters are necessary. The performance of these controllers is based on how accurate the known model and known parameters are used in their design procedures, which in turn the design processes are time-consuming and much labour is acquired to identify the accurate parameters, which present barriers to their practical use.

In the past decades, the first NCTF control has been proposed as a practical controller for point-to-point positioning system and was examined with a rotary mechanism [10]. In the year 2009, the continuous motion nominal characteristic trajectory following (CM NCTF) controller has been proposed as a high performance and simple control structure to a DC ball screw mechanism [11]. The main highlight of this controller is its simple control structure as compared with the other advanced controllers. Besides that, the procedure to design an NCTF controller is much simpler and easy to understand. It does not require an exact model or parameter identification of the plant which sometimes troublesome the researchers. A common pulse input is able to drive the DC driven mechanism easily and stop smoothly in the open-loop experiment, however, it is not the same to an AC driven mechanism. Therefore, in this paper, we do something different in modifying the input signal to drive the mechanism in the open-loop experiment.

In the year 2010, the positioning performance of the CM NCTF control was validated with a non-contact mechanism [12]. It proved that the design procedure of the NCTF controllers is independent of the friction characteristic. In 2013, the effectiveness of the CM NCTF controller was evaluated using the 1-DOF rotary system, which is driven using a DC servo motor [13]. The third generation, Acceleration Reference-Continuous Motion NCTF (AR-CM NCTF) controller was proposed in the year 2010, and its effectiveness was clarified using non-contact [14] and contact mechanisms [15, 16]. In the year 2015, Chong and Sato have reviewed and summarized the applicability of the NCTF controllers for several typical positioning systems that widely used in industries [17].

The main goal of this paper is to examine and clarify the usefulness of the CM NCTF control to a ball screw mechanism that driven using an AC servo motor. AC servo motor produces higher acceleration as compared to DC motor. By using a general pulse input, it may not suitable to decelerate the mechanism before stopping. Hence, a suitable input signal is proposed in this paper, which is able to produce sufficient rapid and smooth response during deceleration motion in the open-loop experiment. The open-loop responses that used to construct nominal characteristic trajectory (NCT) are important because it has significant influences on the reference following characteristic of the control system. Experiments in point-to-point (PTP) and tracking motion in difference axis will be conducted in order to validate the effectiveness of the CM NCTF control system.

The rest of this paper is written as follows: Section 2 describes the experimental setup and dynamic model of the research. In section 3, the control structure of the CM NCTF control system and its design procedure are discussed. The performance of CM NCTF is validated and discussed in section 4. Lastly, the remark conclusion and future studies are made.

2. System Description

Figure 1 shows the AC-driven *X*-*Y* ball screw mechanism that used to examine the usefulness of the CM NCTF controller in this research. The mechanism is driven by an AC servo motor (model: MSMD022P1U) through ball screws with a 5 mm pitch. The lead of the ball screw is 1.25 mm/rev. Each motor is controlled independently by the same servo driver. The maximum travel range of the table is 175 mm for each *X* and *Y* axes.

An incremental encoder with the resolution of 0.5 μm/pulse is used to measure the feedback position of the mechanism. The controller sampling frequency is 1 kHz. The velocity in this research is obtained by applying a backward difference algorithm to the measured displacement. The structure of the *X*-axis and the *Y*-axis are almost similar, except the X-axis is heavier in weight. The *Y*-axis of the *X*-*Y* ball screw mechanism is placed on top of the X-axis as shown in Fig. 1. The *Y*-axis only sustains the mass of the moving table (3.11 kg), but for the *X*-axis, it sustains the masses of both *X* and *Y* tables (total mass 16.71 kg).

The macrodynamic model of a one-axis ball screw mechanism is shown in Fig. 2. In this research, only macrodynamic of the mechanism is considered in the plant modelling. The one-axis ball screw mechanism is assumed to have a damped mass and an AC servo motor. This generic configuration is the same as those of a large number of positioning mechanism used in industry.

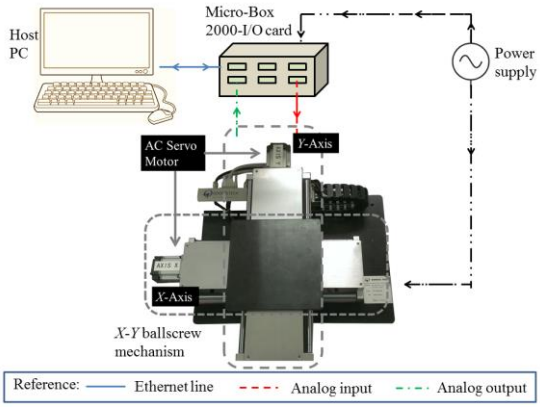

Fig. 1. AC-driven *X*-*Y* ball screw mechanism.

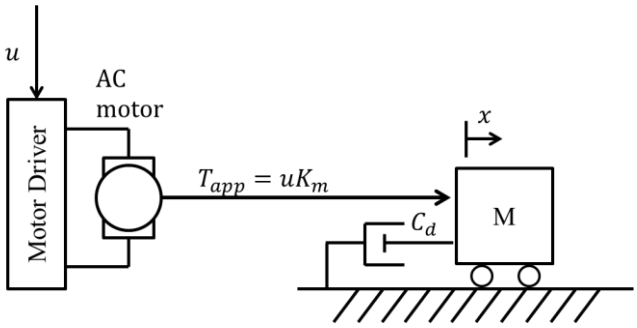

Fig. 2. Dynamic model of ball screw mechanism (macrodynamic characteristic).

The NCTF controller parameter is derived based on the linear macrodynamic model, named as a simplified object model, as shown in Eq. (1):

$$M\ddot{x}(t) + C_d\dot{x}(t) = K_m u(t) \tag{1}$$

$$\ddot{x}(t) + \alpha \dot{x}(t) = Ku(t) \tag{2}$$

which leads to the transfer function of the simplified object model as:

$$\frac{X(s)}{U(s)} = \frac{K}{s(s+\alpha)} \tag{3}$$

The value of $u(t)$ is constant with amplitude u_r and becomes zero after t_f ($t_a + t_b$) (see Fig. 7), parameter K is derived as:

$$K = \frac{\beta x_f}{u(t) t_f} \tag{4}$$

where u represents the input voltage, x_f is denoted as the final displacement, and t_f represents as the final stopping position of the mechanism. In this research, the input voltage, $u(t)$ is set at 5 V. The t_f and x_f are obtained experimentally which are equivalent to 0.28 s and 28.62 mm, respectively.

3. Continuous Motion NCTF Control System

The continuous motion (CM) NCTF controller is the second generation of the NCTF controller [11]. The NCTF controller is modified in order to improve performance in continuous motion. The structure and design procedure of the CM NCTF control remain simple and straightforward.

CM NCTF control system structure

Figure 3 illustrates the control structure of the CM NCTF controller. The CM NCTF controller is composed of a nominal characteristic trajectory (NCT) element and a Proportional and Integrator (PI) compensator. The NCT works as a virtual reference error rate for the object to follow and is expressed on a phase plane. The NCT is constructed using the object responses during the open-loop experiment and the inclination at the origin of the NCT is referred to as β. On the other hand, the PI compensator controls the velocity of the mechanism in order to make the mechanism follows the NCT and finishes at the origin. When the object stops at the origin, it means the end of the positioning motion. The PI compensator is designed based on a practical stability limit that obtained experimentally [18]. The detail of the design procedure for the CM NCTF controller will be discussed in the next sub-section.

The signal $u_p(t)$ represents the difference between the actual error rate ($\dot{e}$) and virtual error-rate of the NCT (e_n). If the value of $u_p(t)$ is equal to zero, then the object motion is perfectly following the NCT. The PI compensator is used to control the object motion to follow the NCT to the origin, so the value of $u_p(t)$ becomes zero. In point-to-point positioning, if the e is large, it will cause a large $u_p(t)$, and the mechanism may not sufficiently follow the NCT. However, the mechanism may demonstrate promising performance in continuous motion, because the controller acts near to the reference, which the actions that far from the reference becomes not important.

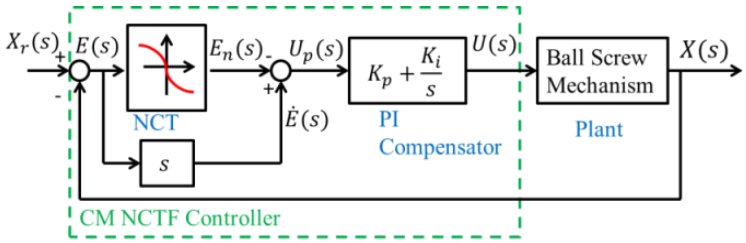

Fig. 3. Control structure of continuous motion nominal

The objective of the NCTF controller is to make the object motion to follow the NCT and ended at the origin. In the NCTF control system, the object motion is divided into two phases as shown in Fig. 4, which are reaching phase and following phase. In the reaching phase, the object motion is controlled by the PI compensator in order to reach the NCT path as fast as possible. Then, in the following phase, the PI compensator will control the object motion to follow the NCT and ends at its origin on the phase plane, which represents the end of the positioning motion.

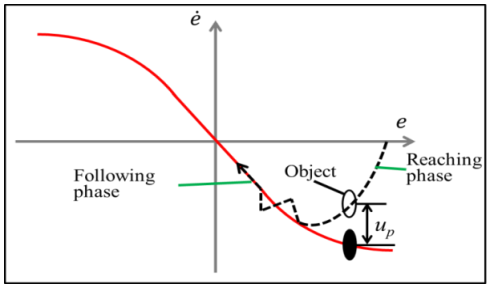

Fig. 4. Reaching phase and following phase in NCT.

3.2. Design procedure

The design procedure of the NCTF control system is simple and comprised of three major steps:

i The mechanism is driven in open-loop and the displacement and velocity responses are measured;

ii The NCT is constructed on a phase plane using the displacement and velocity responses of the mechanism during deceleration in the open-loop experiment;

iii The PI compensator is designed based on the open-loop responses and NCT information.

Figure 5(a) shows a common pulse input that used to drive a typical mechanism with friction in open-loop which is driven by DC motor [19]. The pulse signal in Fig. 5(a) is not suitable to drive an AC-driven contact-type mechanism in open-loop because AC servo motor tends to produce higher acceleration as compared to DC motor. By using a common pulse input in Fig. 5(a), the mechanism might decelerate too fast before stopping, and it may cause large inclination near the origin of NCT. Due to this, it will deteriorate the accuracy of a control system significantly. Therefore, the common pulse signal is modified at its deceleration part, as shown in

Fig. 5(b). The exponential part at the deceleration before stopping plays an important role because it tends to provide a smooth attenuate motion before stopping.

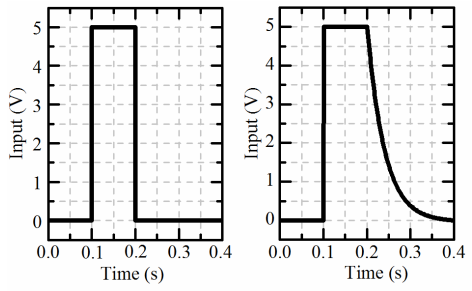

(a) (b)

Fig. 5. Open-loop input signals.

Figure 6 shows the experimental open-loop responses with the input signal in Fig. 5(a) of *Y*-axis. The fast velocity during the deceleration before stopping has caused undesired undershoot response. As we know, the object behaviour before stopping represents the motion characteristic of the mechanism. Therefore, it is necessary to modify the deceleration part of the pulse signal before stopping, in order to provide a smooth attenuation before object stops.

Figure 7 depicts the open-loop responses of the *Y*-axis that commanded by the designed input signal. The designed input signal is the combination of a step and exponential signals. The exponential signal, e^{-at} makes the mechanism attenuate smoothly during deceleration. Considering the damping characteristic of the mechanism, the exponential ratio, a is set as 5. The ratio between t_a and t_b is 1:2 in order to extend the deceleration time. With this, the fast deceleration of the AC servo motor has been solved significantly.

The open-loop responses of the designed input signal are used to construct the NCT. The constructed NCT is shown in Fig. 8. The constructed NCT with inclination near the origin, β equals to 87 s^{-1}. The reference following characteristic of the controller mainly depends on the inclination near the origin, which is important in positioning accuracy. Since the NCT is constructed using the experimental result, therefore the characteristics of the mechanism have been included in the control system.

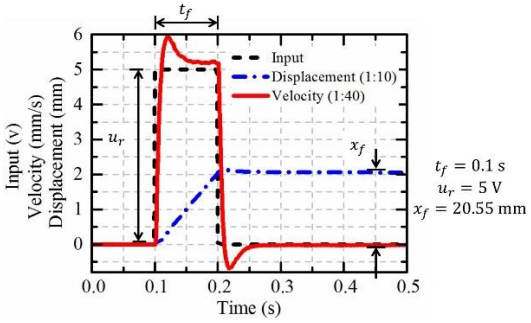

Fig. 6. Experimental open-loop response with common pulse input signal (*Y*-axis).

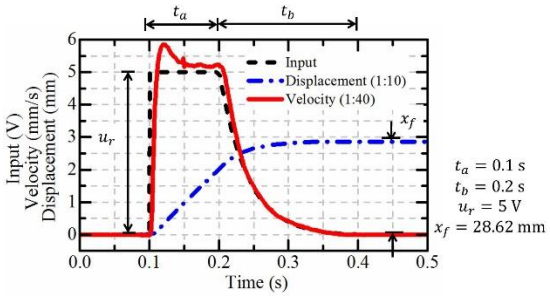

Fig. 7. Experimental open-loop responses with designed input signal (*Y*-axis).

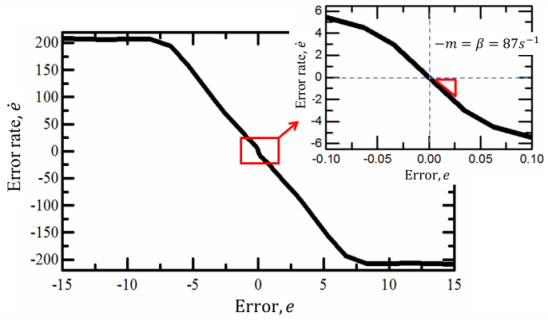

Fig. 8. Constructed NCT and magnified view at origin in *Y*-axis of ball screw system.

PI compensator is designed by considering the stability of the control system. This compensator is designed using the open-loop responses and the NCT information, which are determined experimentally. Proportional gain, K_p and integral gain, K_i are calculated as:

$$K_p = \frac{2\zeta\omega_n}{K}$$
$$K_i = \frac{\omega_n^2}{K} \quad (5)$$

Practical stability limit graph is used to identify the stability of the mechanism. K_p and K_i gains are chosen under the stable region. The practical stability limit is determined by driving the *Y*-axis of the ball screw mechanism with only the constructed NCT and proportional element. The value of proportional gain is increased until oscillations are generated that indicating the occurred of instability.

Figure 9 shows the practical stability limit that constructed experimentally [17]. Three positions under the practical stability limit graph are chosen to investigate the influence of ζ and ω_n to the positioning performance of the CM NCTF control system. Oscillation is expected to occur for the PI compensator at the Q3 position because it is chosen from the unstable region.

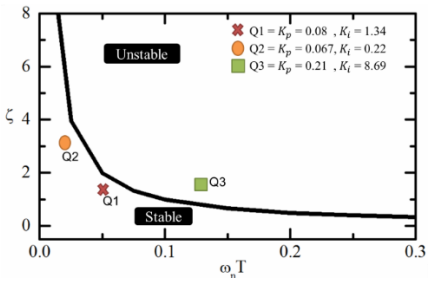

Fig. 9. Practical stability limit.

During the design of the PI compensator, designers are tempted to use large values of $\omega_h T$, where T is the sampling time used in this research. When the value of $\omega_h T$ is too large, the controller will behave as a pure integral controller which may cause instability to the mechanism as proved in [19].

Table 1 shows the controller parameters of each selected position on practical stability limit graph.

Table 1. Compensator parameters.

Controller	Parameters			
	ζ	$\omega_h T$	K_p	K_i
Q1	1.46	0.049	0.08	1.34
Q2	3.03	0.019	0.067	0.22
Q3	1.51	0.124	0.21	8.69

Figure 10 shows the comparative experimental positioning performance for Q1, Q2, and Q3 to step input 1 mm. As expected, oscillation occurs as the PI compensator constructed from Q3. On the other hand, Q2 with larger ζ has demonstrated smaller overshoot as compared to Q1, but Q1 has shown shorter rising time as compared to Q2. For the rest of the experiments in this paper, the Q1 is selected as the PI compensator gains.

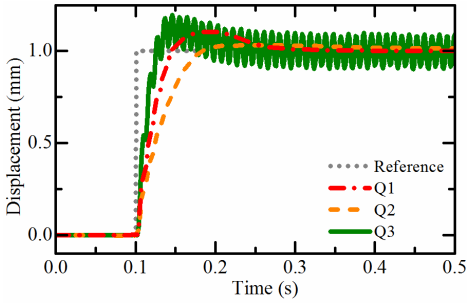

Fig. 10. Experimental point-to-point motion results.

4. Performance Evaluation

In this research, experiments in point-to-point (PTP) and tracking motion will be conducted in order to validate the effectiveness of the CM NCTF control system. Point-

to-point performances with difference amplitude of step input (5 mm and 10 mm) are used to command the mechanism. In addition, tracking performance with different amplitudes (0.1 mm and 10 mm) and frequencies (0.1 Hz and 5 Hz) are used to command the mechanism. PI-D controller is designed to be compared with the CM NCTF controller because this controller has a similar control structure with the CM NCTF controller. The control structure of PI-D controller is shown in Fig. 11.

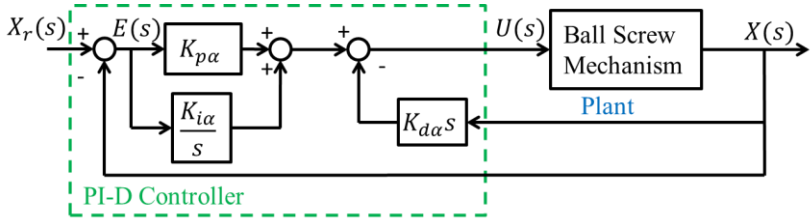

Fig. 11. Control structure of PI-D controller.

The PI-D controller is designed by using the *Y*-axis of the ball screw mechanism. The $K_{p\alpha}$, $K_{i\alpha}$ and $K_{d\alpha}$ gains of the PI-D controller are fine-tuned at step input 1 mm to have similar positioning performance as the CM NCTF control. Figure 12 shows the comparative step responses of both controllers at 1 mm reference input. The results show that PI-D controller is better than the CM NCTF controller, therefore these parameters are chosen for the rest of the experiments.

Table 2 shows the controller parameters of both controllers.

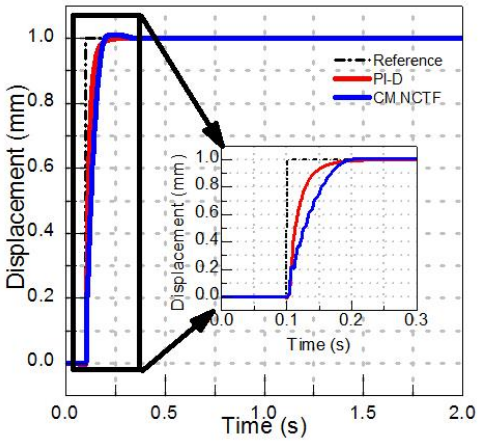

Fig. 12. Comparative experimental step responses to 1 mm of the CM NCTF and PI-D controls.

Table 2. Comparative controller parameters.

Controller	Parameters			
	β (s^{-1})	K_p	K_i	K_d
CM NCTF	87	0.08	1.34	-
PI-D	-	3.00	0.80	0.03

The X-axis mechanism is required to sustain 5.4 times larger mass than the *Y*-axis mechanism. The loaded mechanism produces a narrow pitch noise during a translation. Figure 13(a) shows the tracking error of CM NCTF control for *X*-axis.

The result illustrates the severe accuracy problem, which is caused by the resonant noise when the X-axis is commanded by a sinusoidal input at amplitude 0.1 mm, frequency 0.1 Hz. The measured resonant frequency in Fig. 13(a) is 9 Hz. Hence, a notch filter is included in the control structure for the *X*-axis. A notch filter with ζ_α = 1.47 and $\omega_{n\alpha}$ = 49.07 rad/sec is designed to filter the noise occurred. Figure 13(b) presents the tracking error of the CM NCTF control system for *X*-axis with the inclusion of a notch filter. It can be obviously seen that the error of the system has been reduced to 1 μm. Eq. (6) shows the equation of the designed notch filter.

$$G_{notch}(s) = \frac{s^2 + 2\zeta_\alpha \omega_{n\alpha} s + \omega_{n\alpha}{}^2}{(s + \omega_{n\alpha})^2} \tag{6}$$

4.1. Point-to-point performance

The point-to-point performance of the CM NCTF and the PI-D controllers were examined with the *X*-*Y* AC drive ball screw mechanism. The step inputs with amplitude 5 mm and 10 mm are used to command the mechanism in point-to-point motion. Figures 14 and 15 illustrate the comparative experimental positioning results of both controllers for *X*-axis and *Y*-axis.

As observed, the CM NCTF control system demonstrates better motion accuracy than the PI-D control system for both *X*-axis and *Y*-axis. The CM NCTF control has reduced the motion error to less than 0.5 μm (approaching zero), but the PI-D noted the motion error that larger than 5 μm. The quantitative transient responses of both controllers are shown in Table 3. The CM NCTF controller has succeeded to compensate for the steady-state error (e_{ss}) to zero, while the PI-D controller has a steady-state error that larger than 5 μm for both *Y*-axis and *X*-axis.

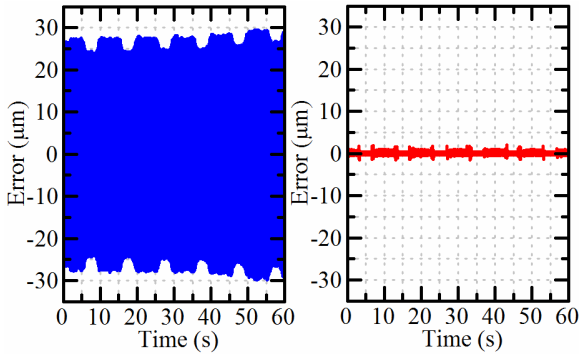

Fig. 13. Experimental tracking performance that commanded by sinusoidal reference input at amplitude 0.1 mm and frequency 0.1 Hz using *X*-axis (a) without; and (b) with the designed notch filter.

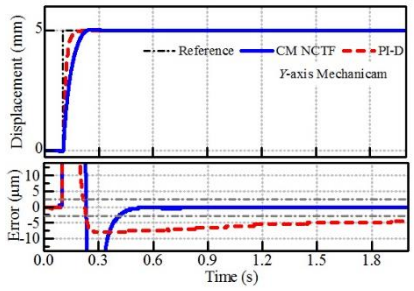

(a) *Y*-axis

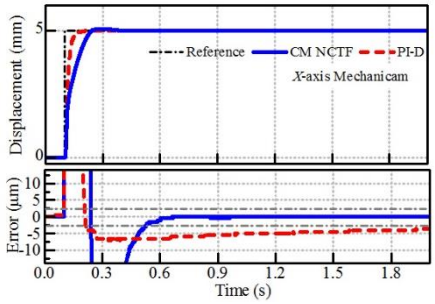

(b) *X*-axis

Fig. 14. Experimental point-to-point positioning performances with step height.

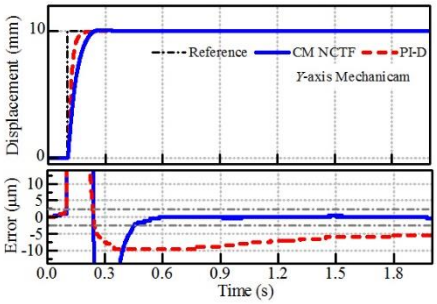

(a) *Y*-axis

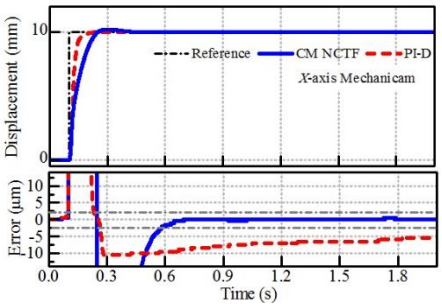

(b) *X*-axis

Fig. 15. Experimental point-to-point performances with step height 10 mm for (a) *Y*-axis; and (b) *X*-axis.

Table 3. Experiment transient response of CM NCTF and PI-D controllers for *Y*-axis and *X*-axis.

Controller	Amp (mm)	*Y*-axis		*X*-axis	
		OS (%)	e_{ss} (μm)	OS (%)	e_{ss} (μm)
CM NCTF	**5.00**	$7.6x10^{-1}$	0.00	2.23	0.00
	10.00	$9.4x10^{-1}$	0.11	1.59	0.00
PI-D	**5.00**	$1.6x10^{-1}$	$1.0x10^{1}$	$1.4x10^{-1}$	7.0
	10.00	$1.0x10^{-1}$	$1.0x10^{1}$	$1.1x10^{-1}$	6.0

Experimental closed-loop frequency responses of both controllers for *Y*-axis and *X*-axis are shown in Fig. 16. The experimental bandwidth of the PI-D controller in *Y*-axis and *X*-axis is recorded as 9.87 Hz and 9.90 Hz respectively. In addition, the experimental bandwidth for the CM NCTF controller is expected to happen at around 10 Hz. The closed-loop bandwidth of both controllers is close to each other, therefore the difference in rising time is not significantly found.

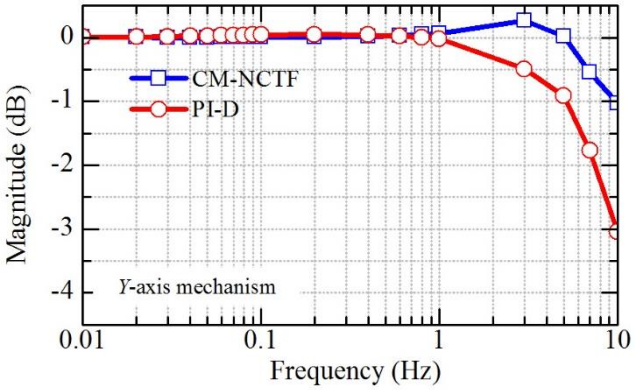

(a) *Y*-axis

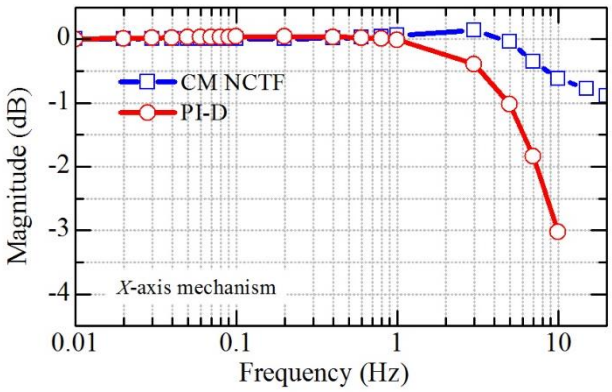

(b) *X*-axis

Fig. 16. Experimental closed-loop frequency response with (a) *Y*-axis; and (b) *X*-axis.

4.2. Tracking performance

A sinusoidal input is used to evaluate the effectiveness of the CM NCTF controller in continuous motion. Figure 17 shows the experimental magnitude plot of open-loop response with Y-axis mechanism. The gain crossover frequency, f_b which is also the bandwidth of the loop gain exceeding 0 dB, at 4.4 Hz. The tracking system at 3-dB bandwidth, f_{bw} which is typically from 1.3 f_b to 1.7f_b, is identified with the reading 6.6 Hz. In order to prevent the mechanism from reaching the unstable region, the experiments that will be carried out to evaluate the effectiveness of the CM-NCTF controller is set at the value that smaller than 6 Hz.

In this experiment, two frequencies are used to command the mechanism, which is 0.1 Hz and 5 Hz. In each frequency, two amplitudes are used to examine the controller, which are 0.1 mm and 10 mm. The maximum peak error is calculated using Eq. (7), where x_r is the reference input and x is the output displacement.

$$e_{\max} = \max |x_r - x| \tag{7}$$

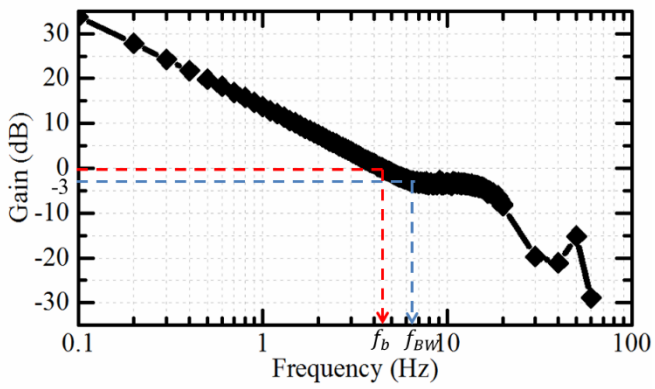

Fig. 17. Experimental open-loop magnitude plot of *Y*-axis.

Figure 18 shows the tracking performance of the CM NCTF and PI-D controllers for Y-axis and X-axis. The amplitude of the sinusoidal input is 0.1 mm with the frequency of 0.1 Hz. In the case of *Y*-axis, the maximum motion error e_{max} is 0.8μm and the PI-D controller is 4.0 μm. The motion error of the CM NCTF controller is 5 times smaller as compared to the PI-D controller. On the other hands, the *X*-axis, which the load is heavier, the motion error of the CM NCTF controller is 1.8 times smaller than the motion error of the PI-D controller.

Figure 19 shows the experimental result with the sinusoidal input of amplitude 10 mm and the frequency remains at 0.1 Hz. In *Y*-axis, the e_{max} of the CM NCTF controller is 16 times smaller than the PI-D controller, where the e_{max} of the CM NCTF controller is 7.1 μm and 110.8 μm for the PI-D controller. For the case of *X*-axis, the CM NCTF controller performs 19 times better tracking performance than the PI-D controller, where the e_{max} of the CM NCTF controller and PI-D controller are 6 μm and 116.5 μm respectively. The frequency of the sinusoidal input is varied in order to examine the adaptability and sensitivity of the CM NCTF controller to the change of reference input.

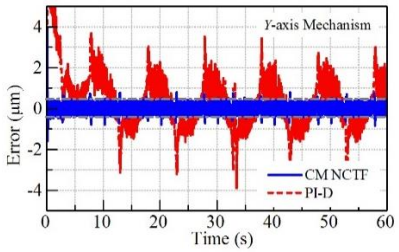

(a) *Y*-axis

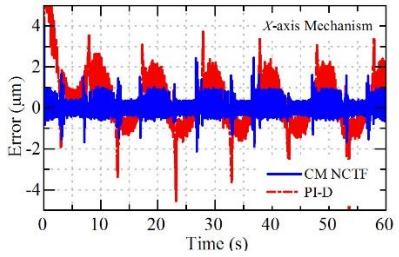

(b) *X*-axis

Fig. 18. Comparative experimental tracking performance of CM NCTF and PI-D controllers (sinusoidal input: amplitude = 0.1 mm, frequency = 0.1 Hz) for (a) *Y*-axis; and (b) *X*-axis.

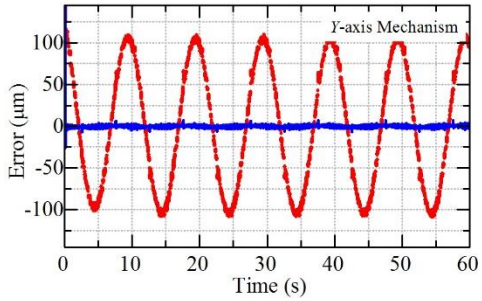

(a) *Y*-axis

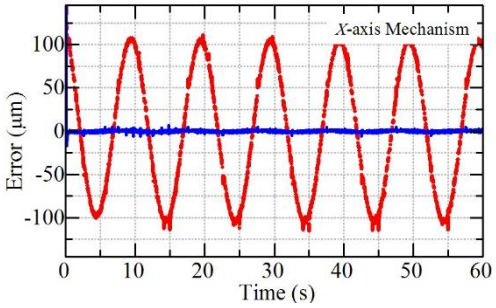

(b) X-axis

Fig. 19. Comparative experimental tracking performances of CM NCTF and PI-D controllers (sinusoidal input: amplitude = 10 mm, frequency = 0.1 Hz) for (a) *Y*-axis; and (b) *X*-axis.

The frequency of the sinusoidal input is increased to 5 Hz (faster velocity). Figure 20 shows the tracking performance of the CM NCTF and PI-D controllers for *Y*-axis and *X*-axis with sinusoidal input at 0.1 mm. The motion error of the CM NCTF controller is 2.6 times smaller than the PI-D controller for *Y*-axis. On the other hands, the motion error of the CM NCTF and PI-D controllers for *X*-axis is 17.2 μm and 72.7 μm respectively, which the CM NCTF controller has shown motion accuracy 4.2 times better than the PI-D controller. By referring to Fig. 16, it is proven that the CM NCTF controller is capable to perform faster response than the PI-D controller.

Figure 21 shows the experimental result with the sinusoidal input of amplitude 10 mm while the frequency is maintained at 5 Hz. For *Y*-axis, the CM NCTF controller has demonstrated the motion error that 2.7 times smaller than the PI-D controller, where the e_{max} of the CM NCTF and PI-D controllers is 1.8 mm and 4.9 mm, respectively. For the case of *X*-axis, the CM NCTF controller performs tracking the performance of that 3.4 times better than the PI-D controller. With the experimental results, we can see that the CM NCTF control has demonstrated significant characteristic in compensating tracking error in comparison to the linear controller, PI-D control. Besides, it can be seen that the tracking performance for the *X*-axis is better than the *Y*-axis in all the cases of frequencies. It can be explained by the existing of the notch filter in the control structure to filter the noise.

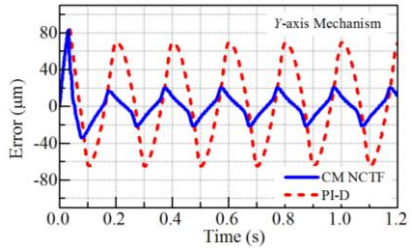

(a) *Y*-axis

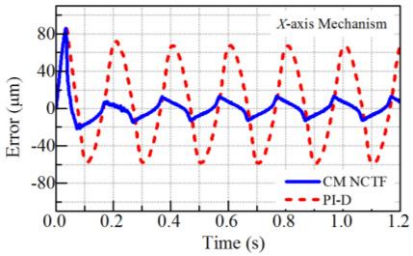

(b) *X*-axis

Fig. 20. Comparative experimental tracking performances of CM NCTF and PI-D (sinusoidal input: amplitude = 0.1 mm, frequency = 5 Hz) for (a) *Y*-axis; and (b) *X*-axis.

4.3. Sensitivity analysis

Sensitivity analysis is needed in order to evaluate the robust performance of the CM NCTF controller. When the sensitivity of the system is low, the influence of the disturbance to the control system is small. In order to reduce the influence of disturbance, the magnitude of the controller should be large over the range of frequencies. System sensitivity is the ratio of the change in a system transfer

function to the change of a process transfer function or parameter for a small incremental change. The system sensitivity, $S(s)$ is shown in Eq. 8, where $R(s)$ is denoted as the reference signal, $E(s)$ is denoted as the error signal, $D(s)$ is the disturbance signal, $Y(s)$ is the output signal, $G_c(s)$ is the controller transfer function, $G_p(s)$ is the plant transfer function, and $H(s)$ is the feedback transfer function.

$$S(s) = \frac{E(s)}{R(s) - D(s)} = \frac{1}{1 + G_c(s)G_p(s)} \tag{8}$$

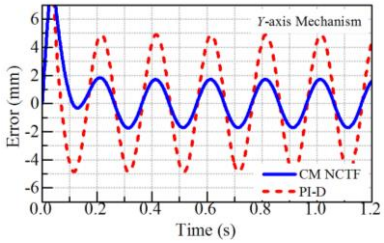

(a) *Y*-axis

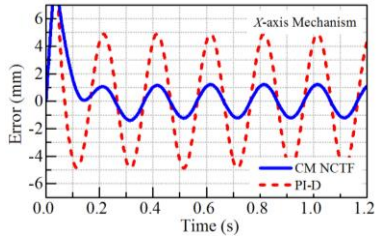

(b) *X*-axis

Fig. 21. Comparative experimental tracking performances of CM NCTF and PI-D (sinusoidal input: amplitude = 10 mm, frequency = 5 Hz) for (a) *Y*-axis, and (b) *X*-axis.

Figure 22 shows the simulated frequency response of sensitivity, $S(s)$ for all controllers. At low frequency, the CM NCTF controller shows the largest magnitude as compared to PI-D controller. Hence, the influence of disturbance to the performance of CM NCTF controller is smaller as compared to the PI-D controller. Moreover, the experimental results also prove that of the CM NCTF controller is less sensitive to the change of input amplitudes, frequencies and mass variation.

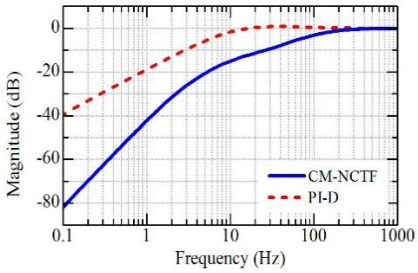

Fig. 22. Simulated frequency response of sensitivity, *S(s)*. for sensitivity analysis of the CM NCTF and PI-D controllers.

5. Conclusions

In this paper, the positioning and tracking performance of the CM NCTF control system were clarified using an AC driven *X-Y* ball screw mechanism. In order to consider the suitability inclination at the origin of NCT, the mechanism deceleration motion before stopping is necessary to be considered. For that, a suitable input signal is designed to produce sufficient rapid and smooth response during deceleration motion in the open-loop experiment. The design of the PI compensator that based on the practical stability limit is important to consider the stability of the control system. In the point-to-point motion, the CM NCTF controller has successfully compensated the steady state error to zero. In tracking motion, the CM NCTF controller has demonstrated the smallest tracking error as compared to the PI-D controller as the input signal varies. The motion error of the CM NCTF controller is reduced, although the weight of the mechanism is increased 5.4 times. Although the CM NCTF controller has shown slightly larger overshoot in point-to-point motion, the CM NCTF controller has shown better tracking performance than the PI-D controller. Overall, the CM NCTF controller has successfully to demonstrate promising positioning and robust performance.

Nomenclatures

C_d	Damping coefficient, Ns/m
$\dot{e}$	Actual error rate, mm/s
e	Positioning and tracking errors, m
e_n	Virtual error rate of NCT, mm/s
K_i	Integral gain (CM NCTF)
$K_{i\alpha}$	Integral gain (PI-D)
K_m	Force constant, N/A
K_p	Proportional gain (CM NCTF)
$K_{p\alpha}$	Proportional gain (PI-D)
M	Table mass, kg
T	Sampling time, s
t_f	Time to reach final displacement, s
$u(t)$	Input voltage, V
u_p	Difference between the actual error rate and virtual error rate of NCT
$x(t)$	Table displacement, mm
$x_f(t)$	Final displacement, mm
x_r	Reference input, mm

Greek Symbols

ζ	Damping ratio
ω_n	Natural frequency, rad/s

Abbreviations

AR	Acceleration Reference
CM	Continuous Motion
NCT	Nominal Characteristic Trajectory
NCTF	Nominal Characteristic Trajectory Following
PID	Proportional Integral Derivative
PTP	Point-to-Point

References

1. Shigemasa, T.; Negishi, Y.; and Baba, Y. (2013). A TDOF PID control system design by referring to the MD-PID control system and its sensitivities. *Proceedings of the European Control Conference.* Zurich, Switzerland, 3937-3942.
2. Guo, J.; Wu, G.; and Guo, S. (2015). Fuzzy PID algorithm-based motion control for the spherical amphibious robot. *Proceedings of the IEEE International Conference on Mechatronics and Automation (ICMA)*. Beijing, China, 1583-1588.
3. Abdullah, L.; Jamaludin, Z.; Maslan, M.N.; Jamaludin, J.; Halim, I.; Rafan, N.A.; and Chiew, T.H. (2015). Assessment on tracking performance of cascade P/PI, NPID and NCasFF controller for precise positioning of XY table ballscrew drive system. *Procedia CIRP*, 26, 212-216.
4. Xu, J.; Qiao, M.; Wang, W.; and Miao, Y. (2011). Fuzzy PID control for AC servo system based on stribeck friction model. *Proceedings of the 6th International Forum on Strategic Technology*. Heilongjang, China, 706-711.
5. Zhang, C.; and Chen, Y. (2016). Tracking control of ball screw drives using ADRC and Equivalent-Error-Model Based Feedforward Control. *IEEE Transactions on Industrial Electronics*, 63(12), 7682-7692.
6. Lin, C.-J.; and Lee, C.-Y. (2011). Observer-based robust controller design and realization of a gantry stage. *Mechatronics*, 21(1), 185-203.
7. Li, Z.; Chen, J.; Zhang, G.; and Gan, M. G. (2011). Adaptive robust control for DC motors with input saturation. *IET Control Theory and Applications*, 5(16), 1895-1905.
8. Lu, C.H.; and Hwang, Y.R. (2012). Hybrid sliding mode position control for a piston air motor ball screw table. *ISA Transactions*, 51(3), 373-385.
9. Fernandez-Gauna, B.; Ansoategui, L.; Etxeberria-Agiriano, I.; and Grana, M. (2014). Reinforcement learning of ball screw feed drive controllers. *Engineering Applications of Artificial Intelligence*, 30, 107-117.
10. Wahyudi; K.; Sato, K.; and Shimokohbe, A. (2003). Characteristics of practical control for point-to-point (PTP) positioning systems. *Precision Engineering*, 27(2), 157-169.
11. Sato, K.; and Maeda, G.J. (2009). A practical control method for precision motion - improvement of NCTF control method for continuous motion control. *Precision Engineering*, 33(2), 175-186.
12. Chong, S.-H.; and Sato, K. (2010). Practical controller design for precision positioning, independent of friction characteristic. *Precision Engineering*, 34(2), 286-300.
13. Rozilawati, M.N.; and Chong, S.-H. (2013). Positioning control of a one mass rotary system using NCTF controller. *Proceedings of the 2013 IEEE International Conference on Control System, Computing and Engineering*. Mindeb, Malaysia, 381-386.
14. Chong, S.-H.; Hashimoto, H.; and Sato, K. (2011). Practical motion control witn acceleration reference for precision motion - new NCTF control and its application to non-contact mechanism. *Precision Engineering*, 35(1), 12-23.

15. Chong, S.-H.; and Sato, K. (2014). Practical and robust control for precision motion: AR-CM NCTF control of a linear motion mechanism with friction characteristics. *IET Control Theory and Applications*, 9(5), 745-754.
16. Chong, S.-H.; and Sato, K. (2011). Practical and robust control for precision positioning systems. *Proceedings of the IEEE International Conference on Mechatronics*. Istanbul, Turkey, 961-966.
17. Chong, S.-H.; and Sato, K. (2015). Nominal characteristics trajectory following control as practical controller: a review. *Proceedings of the 41st Annual Conference of the IEEE Industrial Electronics Society*. Yokohama, Japan, 4790-4795.
18. Hee, W.-K.; Chong, S.-H.; and Che Amran, A. (2014). Selection of PI compensator parameters for NCTF controller based on practical stability limit. *IEEE International Conference on Control System, Computing and Engineering*. Batu Ferringgi, Malaysia, 674-679.
19. Maeda, G.J.; and Sato, K. (2008). Practical control method for ultra-precision positioning using a ballscrew mechanism. *Precision Engineering*, 32(4), 309-318.